

On the volume change in Co–Ni–Al during pseudoelasticity

S. Dilibal^a, H. Sehitoglu^{a,*}, R.F. Hamilton^a, H.J. Maier^b, Y. Chumlyakov^c

^a University of Illinois, Department of Mechanical Science and Engineering, 1206W. Green St., Urbana, IL 61801, USA

^b University of Paderborn, Lehrstuhl f. Werkstoffkunde, D-33095 Paderborn, Germany

^c Siberian Physical Technical Institute, Revolution Sq.1, Tomsk, 634050, Russia

ARTICLE INFO

Article history:

Received 17 August 2010

Received in revised form

15 December 2010

Accepted 16 December 2010

Available online 23 December 2010

Keywords:

Volume change

Pseudoelasticity

Critical stress

Phase transformation

Digital image correlation

Hysteresis

ABSTRACT

CoNiAl alloys are a new class of shape memory alloys, which exhibit pseudoelastic strains as high 6% over a broad range of temperatures. Based on the crystallographic lattice constants, a substantial volume change upon transformation is expected at the mesoscopic level, yet it has not been measured previously. Transformation strains are established in three mutually orthogonal directions in the [001]-oriented CoNiAl single crystals under compression. Experiments reveal that the transformation volume change is approximately 2% based on determination of strains on transformed and untransformed locations. Despite the high volumetric strain, the pseudoelastic stress–strain response represents full recoverability with small stress hysteresis. Additional factors that influence pseudoelasticity behavior are discussed particularly the $M_d - A_f$ interval and the flow resistance, which are both higher for CoNiAl compared to other shape memory alloys.

© 2010 Elsevier B.V. All rights reserved.

1. Introduction

New shape memory alloys such as CoNiAl have considerable potential, exhibiting a wide pseudoelastic window, small hysteresis and high temperature recoverability [1–4]. It is important to understand the reasons for the favorable response of CoNiAl despite the substantial volumetric strain. In previous work, both compressive response and tensile behavior [1] with large pseudoelastic strains near 6% under tension and 3.5% in compression have been reported. The outstanding feature of CoNiAl is that it undergoes a finite volume change while traditional shape memory materials exhibit very small volume change during the transformation [5]. It is well known dating back to Hornbogen and Skrotzki [6] that volume change should curtail the shape memory effect. Hornbogen also identified the transformation shear and plastic flow resistance as two other factors. These two factors are manifested via the magnitude of the transformation shear vector \mathbf{b} , and also the high M_d temperatures (M_d is the temperature above which martensite cannot be stress-induced) relative to the austenite finish temperature A_f . Gross plastic deformation with irreversible plastic strains dominate the mechanical response at temperatures above M_d . Therefore, the higher the M_d temperature, the austenite to martensite transformation could occur at temperatures sufficiently lower than M_d with

limited irreversibilities. Other factors that govern superior SMAs have been proposed more recently [7], one is the intermediate value of the eigenvalue of the lattice transformation tensor. It is known that if the intermediate eigenvalue of the transformation tensor is unity then the austenite–martensite interface is twinless and smaller number of interfaces develop. The reduction in the number of interfaces lowers the dissipation under transformation [8].

A schematic of factors that are important in design of shape memory alloys is given in Fig. 1. In Fig. 1(a) the austenite to martensite transformation is depicted with no volume change, the habit plane normal, \mathbf{m} , and the transformation shear direction, \mathbf{b} , are orthogonal. The magnitude of \mathbf{b} is the transformation shear. The $\det U = 1$ (the determinant of the lattice transformation tensor) corresponds to no volume change. On the other hand, in Fig. 1(b), the transformation occurs with a volume change, in this case $\det U \neq 1$, and \mathbf{m} and \mathbf{b} are no longer orthogonal. In Fig. 1(c), the critical stress versus temperature is shown for a typical shape memory alloy. We note the two separate critical stress curves for martensite. The lower one for temperatures below M_s represents the reorientation and detwinning of the martensite (self-accommodated martensite is formed upon cooling). The upper curve represents the intrinsic resistance of martensite to slip and deformation twinning. The intrinsic martensite resistance is not the reorientation/detwinning curve (black curve below M_s) that is sometimes (and erroneously) classified as the martensite flow stress. The austenite slip resistance is shown in the same figure at temperatures above M_d . The higher the M_d , the higher the slip resistance of the austenite. The increase

* Corresponding author. Tel.: +1 217 333 4112; fax: +1 217 244 6534.
E-mail address: huseyin@uiuc.edu (H. Sehitoglu).

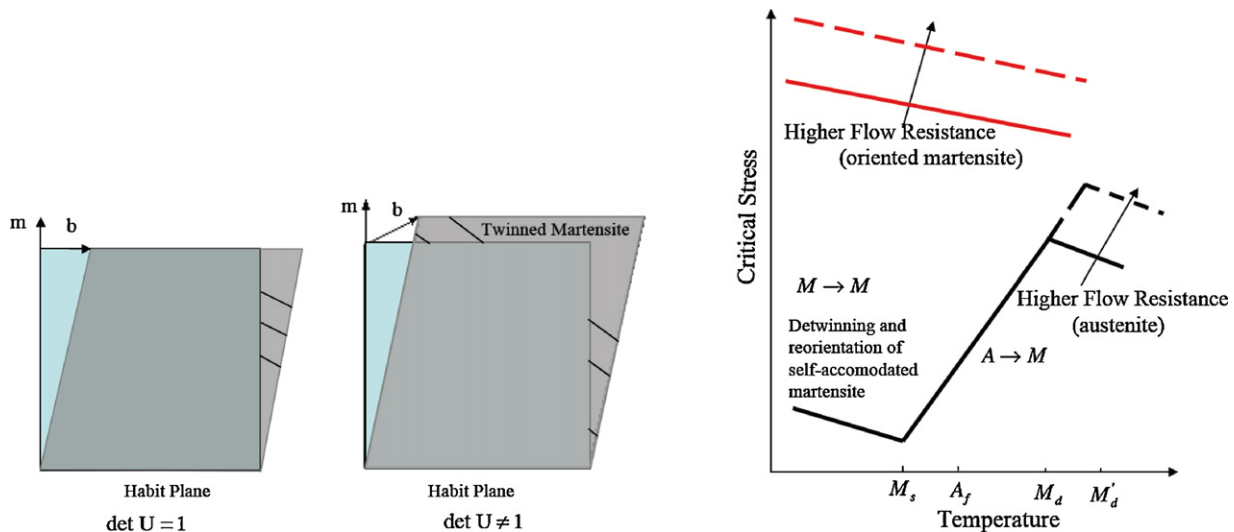


Fig. 1. (a) Schematic of transformation geometry in the presence of pure shear deformation, (b) shear and volumetric expansion, lattice invariant shear is the magnitude of vector **b**, (c) increase in strengthening of the austenite phase limits slip and increases M_d and transformation reversibility.

in M_d to M'_d increases the pseudoelastic temperature interval. To achieve superior pseudoelastic properties the $M_d - A_f$ differential should be high (consequently allowing pseudoelasticity over a wide temperature range); in addition the elevation of austenite and martensite flow stresses facilitates the occurrence for pseudoelasticity.

Another important factor is the ordering of the alloy as pointed out by Ahlers [9]. Most of the engineering shape memory alloys are fully ordered (the order parameter is one). When the alloy is ordered there is a unique pathway for the material to transform back and forth. In the case of CoNiAl, despite the large volume change the material exhibits remarkable pseudoelastic (PE) strain and full recoverability [1–4].

We provide a summary of the det U , transformation shear, the intermediate eigenvalue of the lattice transformation tensor, the M_d and A_f temperatures and the maximum reversible strains for the well known shape memory alloys in Table 1. We analyzed NiTi (cubic to monoclinic) [10], NiTi (cubic to orthorhombic R) [11], NiTiCu (cubic to monoclinic or cubic to orthorhombic depending on Cu content) [12], CuZnAl (cubic to 18R) [5], CuNiAl (cubic to orthorhombic) [5], FeNiGa (cubic to tetragonal) [14], FeNiCoTi

(cubic to tetragonal) [15], and CoNiAl (cubic to tetragonal) [1–4]. The results in Table 1 represent all the shape memory alloys studied by Sehitoglu and co-workers over the years [1,2,4,10–15]. The volume change is small for most shape memory alloys in our list with the exception of CoNiAl. Particularly, we note that in Ni and Cu based shape memory alloys the volume change is considerably smaller than in CoNiAl [1,2,4,10–14]. The theoretical volume change for CoNiAl is as high as 1.8% (using lattice constants from [3]), whereas its magnitude is -0.6% for NiFeGa, -0.35% for NiTi, and lower for most SMAs highlighted in Table 1.

Depending on the alloy there are different number of lattice correspondences, for NiTi the number is twelve while for CoNiAl it is three. The U tensors are constructed from these correspondences and the det U is the same for a given alloy by choosing one of the three to 12 tensors. To determine the transformation shear, we calculate the habit plane and transformation direction for each material and then the magnitude of the vector **b** is determined. We note the magnitude of **b** is in the range 0.0958–0.23. The procedure for all calculations is described in Refs. [10,11].

The CoNiAl alloys possess a remarkably high $M_d - A_f$ differential (only next to NiFeGa) and a transformation shear smaller than most

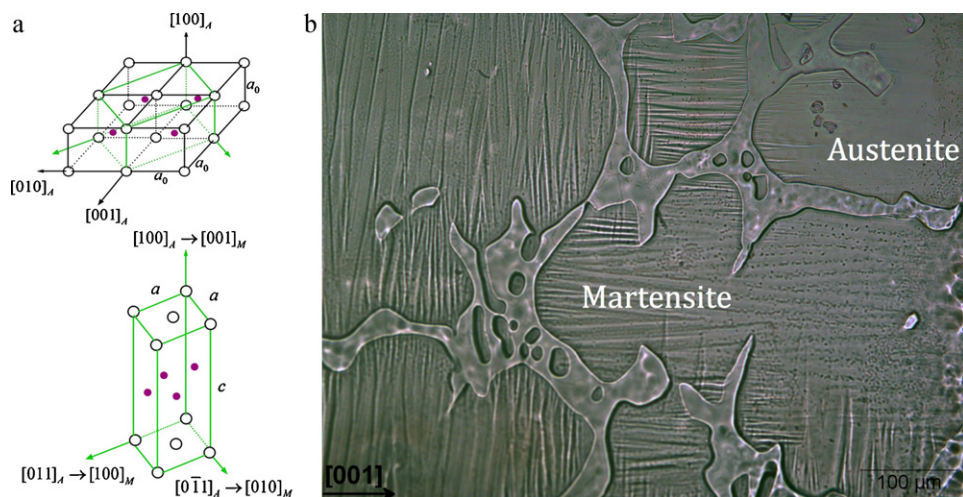


Fig. 2. (a) The unit cells for the austenite to martensite transformation of CoNiAl. The cubic constant has been established from diffraction measurements in our work to be $a_0 = 2.85 \text{ \AA}$ in agreement with Oikawa et al. [16]. The martensitic constants are $c = 3.875 \text{ \AA}$ and $a = 3.139 \text{ \AA}$ from [3], (b) Typical microstructure of CoNiAl alloys showing austenite matrix, martensite plates and the secondary (γ) phase [1,2].

Table 1

A summary of shape memory alloys showing the det U , and temperatures, critical stress (austenite) and maximum transformation strain obtained based on lattice parameters measurements. Experimental values, *, are shown when the theoretical values cannot be reached by experiment.

Shape memory alloy	det U	Intermediate eigen strain	Transformation shear	Temperature hysteresis (°C)	Critical stress (A) MPa	M_d/A_f Temperatures (°C)	Maximum transformation strain	
							Tension	Compression
NiTi (cubic to monoclinic) [10]	0.9965	0.9962	0.13	~30	700–900 (C)	75 to 140/–10 **,#	0.105	–0.064
NiTi (cubic to orthorhombic R) [11]	0.99705	1.0216	0.026	~2	–	–	0.0017 to 0.0051	–0.0026 to –0.0052
NiTiCu (cubic to monoclinic/orthorhombic) [12]	1.0008 1.0128++	0.9895 0.9986++	0.1438 0.097++	~10	500 (C)	100/50	0.0939, –0.057	–0.061, –0.0415
CuZnAl (Cubic to 18R) [5]	0.997 (exp.)	–	0.23	~10	–	30/–25	0.09	–0.09
CuNiAl (cubic to orthorhombic) [5]	0.997	1.023	0.0958	~30	–	–	0.062	–0.082
FeNiGa (cubic to tetragonal) [14]	0.994	0.9354	0.1267	~2	900 (T)	340/30	0.14	–0.062
FeNiCoTi (cubic to tetragonal) [15]	1.0032	1.097	0.1823	~200	850 (T)	475/10	0.03*	–0.015*
CoNiAl (cubic to tetragonal) [1–4]	1.018	0.9614	0.0975	~20	1000–1700 (C)	500/0 to 40#	0.06*	–0.033*

(*) denotes experimental values, (++) cubic to mono/orthorhombic twinless, (**) nickel-rich near equiatomic (composition dependent), (–) rhombohedral angle = 89.4°, (#) depends on the composition and heat treatment, (C) – compression, (T) – tension, (A) – Austenite.

shape memory alloys. For NiTiCu we provide the transformation shear for both the monoclinic and orthorhombic cases. The $M_d - A_f$ differential is rather small for some of the SMAs (such as in FeNiCoTi) while it is very wide for FeNiGa permitting pseudoelasticity over a broad range of temperatures. The critical stress for austenite at the M_d temperature is also provided. We note that obtaining the martensite critical stress (due to mechanical twinning or slip) is far more difficult because the specimen often fractures prior to reaching the martensite flow stress.

In summary, the CoNiAl represents a very unique system that defies the conventional criteria for superior shape memory properties. We explore, in this study, one aspect of this anomaly, namely the volumetric strain change. The use of single crystals allows precise separation of elastic and transformation strains, since elastic constants are also measured. The use of single crystals also results in uniform strain regions, with no intergranular constraint, separated by a transformation front. This sets the stage for precisely measuring the volumetric strain during phase change in transformed regions.

2. Crystallographic background

The CoNiAl alloys undergo a cubic β -phase (B2) to face centered tetragonal austenite (L1₀) transformation. Consequently, three variants are involved in the transformation. The three lattice correspondences (orientation relationships) are shown in Fig. 2(a). The tetragonal unit cell is shown within the cubic supercell on the left. In Fig. 2(a), the Al atoms are at the corners and Co and Ni atoms are in the middle faces. The lattice constants for the cubic phase and for the face centered tetragonal phase are given in the caption to Fig. 2.

There are three lattice correspondences in this case described by the three lattice deformation tensors. The transformation stretch tensor relates the martensite lattice to the austenite crystal. The number of lattice transformation stretch tensors depend on the symmetries between the two lattice and their determinants would be the same for any of the matrices. Precise measurements of lattice constants are given recently by Maziarz et al. [3] as $a_0 = 2.85 \text{ \AA}$, $a = 3.875 \text{ \AA}$, $c = 3.139 \text{ \AA}$. Then, the first transformation

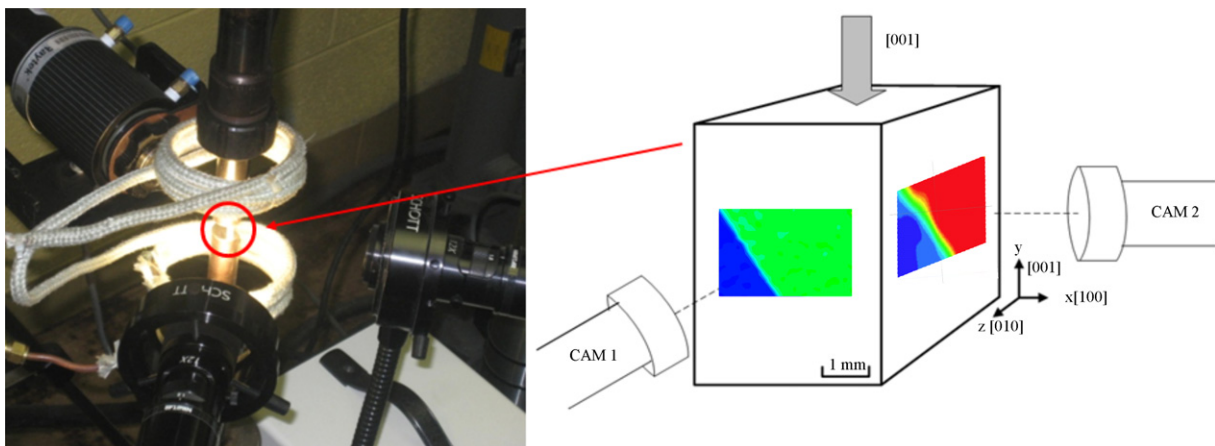


Fig. 3. (a) A photograph of the experimental setup to measure strains on two surfaces of [001] compression specimens (the induction coils are used for heating, ring lights are mounted on the lenses), (b) Schematic indicating the specimen dimensions and the surfaces investigated.

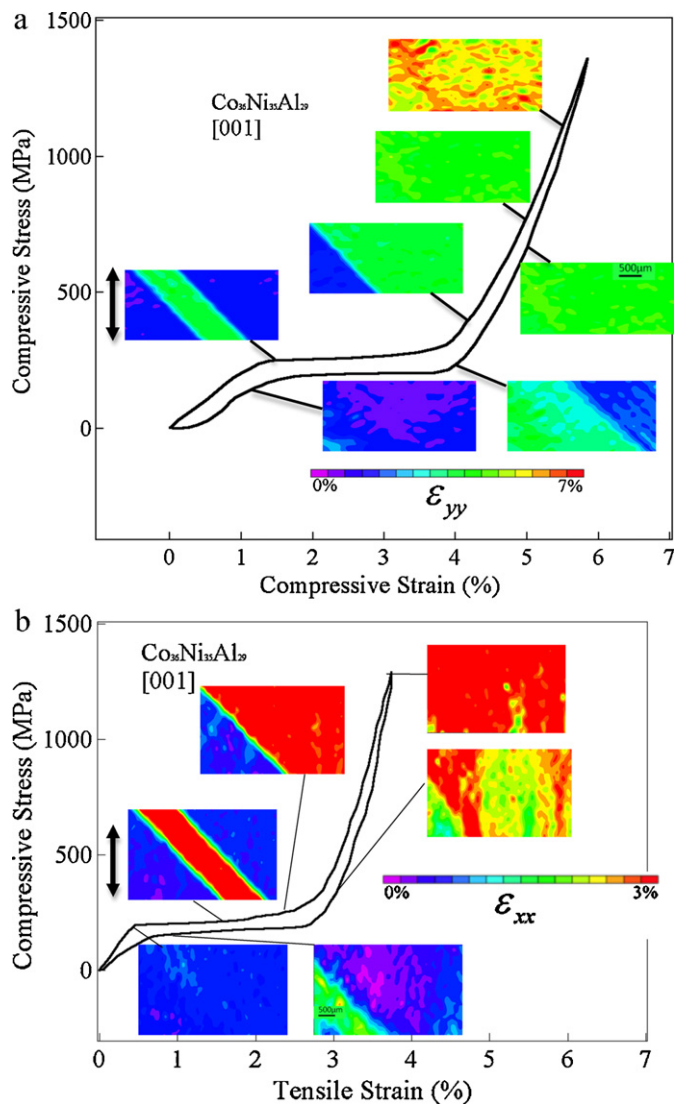


Fig. 4. (a) Pseudoelastic response of [001]-oriented CoNiAl crystals ($T=50^{\circ}\text{C}$) in compression in normal direction (ϵ_{yy}); an expanded view of the plateau region with transformed and untransformed domains are shown in Fig. 5. The loading direction is marked with an arrow. (b) Pseudoelastic response of [001]-oriented CoNiAl crystals ($T=50^{\circ}\text{C}$) in compression in transverse direction (ϵ_{xx}); an expanded view of the plateau region with transformed and untransformed domains are shown in Fig. 5. The loading direction is indicated with an arrow.

stretch tensor is given as $U_1 = \begin{bmatrix} \gamma & 0 & 0 \\ 0 & \eta & 0 \\ 0 & 0 & \eta \end{bmatrix}$ where the lattice constants define the terms $\eta = \frac{a}{\sqrt{2}a_0} = 0.9614$, $\gamma = \frac{c}{a_0} = 1.1014$. Then,

$$U_1 = \begin{bmatrix} 1.014 & 0 & 0 \\ 0 & 0.9614 & 0 \\ 0 & 0 & 0.9614 \end{bmatrix}. \text{ The determinant of this tensor}$$

($=1.018$) provides a measure of lattice volume change, which is 1.8% (also see Table 1). In view of this background, we embarked on an experimental corroboration of the volumetric strain during the deformation experiments. We separate the elastic contributions to the volumetric strain that arises from external stresses and obtained consistent measurements upon repeated experiments.

The microstructure of CoNiAl is shown in Fig. 2(b). It consists of a cobalt rich γ phase and the β matrix (austenite). Due to the existence of the secondary phase ‘networks’ within the matrix as shown in Fig. 2(b), we need to emphasize that the austenite is indeed a single crystal with the same crystallographic orientation throughout

the samples tested. The scale bar shown is $100\ \mu\text{m}$ in Fig. 2(b). The martensite plates are marked within the austenite phase. The γ phase does not undergo phase transformation. This microstructure is typical of CoNiAl examined in early studies, the role of heat treatment on transformation temperatures have been studied earlier [1,2,4].

3. Experimental procedure

Single crystal Co36–Ni35–Al29 (at.%) samples were grown using the Bridgman technique in an inert environment. The dimensions of the rectangular (compression) specimens were $4\ \text{mm} \times 4\ \text{mm} \times 10\ \text{mm}$. The [001] orientation was selected for experiments because of the simpler definition of elastic constants, and ease of orthogonal measurements. The [001] orientation undergoes limited slip because of the lack of easily activated slip systems. This was confirmed in early studies [1,2]. Based on differential scanning calorimetry results at annealing temperatures of 1200°C , 1275°C and 1350°C for annealing times varying from 0.5 h to 48 h, we selected the 1200°C 36 h heat treatment. For this heat treatment the austenite finish temperature is 40°C while the martensite start temperature is 10°C . The material exhibits pseudoelasticity to maximum strains of 6% in tension and 3.3% in compression. In the current work, we conducted cyclic loading experiments in compression with stable stress–strain curves and transformation strains of the order of 3.3%. The lattice constants have been originally reported by Oikawa et al. [16] and detailed measurements were provided recently by Maziarz et al. [3].

The current work is focused on characterizing the spatial and temporal strain changes of phase transformations and specifically the computation of the volumetric strain. The digital image correlation (DIC) was used to obtain full-field strain measurements. We utilized a two lens camera system to simultaneously monitor the vertical, transverse and thickness strains. The setup is shown in Fig. 3. The strains are monitored during the entire loading and unloading. Elastic and transformation strains were extracted from uniformly deformed domains, and the volumetric strains were computed as described later.

In-situ mesoscopic observations were used to investigate the evolution of the transformation. Images were captured with an IMI model IMB-202FT CCD camera (1600×1200 pixels). A Navitar optical lens was used for macroscopic observations at low magnification, which resulted in a resolution of 135 pixels/mm. DIC was performed on images of approximately $1.6\ \text{mm} \times 5\ \text{mm}$ regions of interest to determine the local strain fields during loading and unloading. Full-field measurements of both in-plane displacement components were obtained using DIC. The DIC technique measures displacement fields by tracking features on the specimen surface with a random speckle pattern. Speckle patterns were applied to the surface of polished specimens using an Iwata Micron B airbrush. To perform DIC, a region of interest is selected in the reference image and divided into small square regions called subsets. Each subset represented a square region of approximately $200\ \mu\text{m} \times 200\ \mu\text{m}$. Approximately 17,000 subsets were used to create the strain fields presented. The average pixel intensity in each subset is calculated, and regions with the same intensity are sought in the deformed image. In order to find the location of a deformed subset and its shape change, optimization techniques are employed in which values of displacement and linear displacement gradients of a subset are obtained. For each subset, these values are adjusted until the difference in pixel intensity between the reference and deformed subsets is a minimum. Including higher order displacement gradients had an insignificant effect on the results. The resulting displacement field is then differentiated to obtain the strain field according to a central difference scheme. The nom-

inal strain was calculated by averaging the DIC strain field. The strain fields are subsequently used to determine the fraction of each phase. This is done by comparing the measured strain to theoretical values of strain having accounted for an approximate elastic strain and the transition region between the two phases. Commercially available software (Vic2d) from Correlated Solutions was used to perform the image correlation and the strain calculations.

4. Experimental results

The mechanical response of the CoNiAl alloy at 50 °C is shown in Fig. 4(a) and (b). The single crystal alloy oriented in [001] direction is subjected to compression. In Fig. 4(a) the stress–axial strain response is shown, and in Fig. 4(b) stress–lateral (in xx direction) strain is plotted. In the initial elastic region, we note that some inhomogeneity is observed during elastic deformation (Fig. 4(b) first image). This is believed to be due to the presence of the secondary phase structure. The transformation starts at a stress level near 185 MPa and proceeds over a near plateau region. The deformation occurs by the growth of a single variant (shown as a green band in Fig. 4(a) and as a red band in Fig. 4(b)) that nucleates in the middle of the sample and interfaces grow towards the ends of the specimen. These transformed regions undergo an axial strain of 3.9%. Upon loading above 4% axial strain the transformed regions undergo elastic deformation (shown as yellow and red regions in Fig. 4(a)). Upon unloading reverse transformation occurs in such a way that the region that transformed last now undergoes reverse transformation first. The path of the transformation front upon reversal was not identical to the forward transformation case, as noted in the strain fronts.

The strain fields in the austenite and transforming domains at the plateau stress are shown in Fig. 5. In Fig. 5(a)–(c), the transformed regions are at the right of each figure. The interface separating the untransformed region is diagonal and approximately in the middle of each DIC image. For example, in Fig. 5(a) the strains in the loading direction in the untransformed and transformed regions are -3.95% and -1.1% respectively. We note that as the transformation front proceeds, elastic accommodation occurs with a nearly linear transition zone from the transformed to untransformed (elastic) domains. If there was evidence of accommodation via plastic flow in the vicinity of the interfaces, this would have been apparent from the strain contours.

As the loading is increased the martensite domains grow in expense of the austenite until a fully martensitic structure is reached. It is important that the strain measurements are made far away from the interfaces where there is a transition–elastic accommodation zone. Consequently, we made these measurements in the transformed states away from the phase boundaries to avoid local variations in the strain fields. Even in these cases, the strain fields may not be entirely uniform because of secondary phases and the dendritic structure. The DIC is capable of detecting these small variations, therefore average strains from multiple areas (approximately 10 regions) were obtained to compute the elastic and transformation strains. A method of measuring the volumetric strain ($\Delta V/V$) has been developed as follows. The strain components ε_{xx} , ε_{yy} and ε_{zz} are the axial strain, transverse and thickness strain components respectively (for the martensite phase). The volumetric transformation strain is determined by removing the elastic contribution to the volumetric strain (in the martensite phase) and assuming plastic incompressibility,

$$\Delta V/V^{\text{tr}} = \frac{\Delta V}{V} - \frac{\Delta V}{V^{\text{el}}} \quad (1)$$

where $\Delta V/V$, $\Delta V/V^{\text{el}}$ are the total and elastic component of the volumetric strain and are determined experimentally as $\Delta V/V = \varepsilon_{yy} + \varepsilon_{xx} + \varepsilon_{zz}$ and $\Delta V/V^{\text{el}} = \varepsilon_{yy}^{\text{el}} + \varepsilon_{xx}^{\text{el}} + \varepsilon_{zz}^{\text{el}}$ respectively. For

the case of CoNiAl, we note the difference in the elastic strains in the martensite and austenite (moduli for the martensite is 45 GPa compared to 20 GPa for austenite, see Fig. 4). We also note that the unloading curves have some non-linearity, therefore the unloading curve is idealized as linear (using a secant modulus) until reverse transformation. The elastic constants are then determined from repeated experiments. In some of the experiments, the loading and unloading portions overlapped better and it was easier to define an elastic modulus for martensite. In the case of a tetragonal phase we can describe the elastic constants as $\{\varepsilon_{yy}^{\text{el}} \ \varepsilon_{xx}^{\text{el}} \ \varepsilon_{zz}^{\text{el}}\} = \{S_{11} \ S_{12} \ S_{13}\} \sigma$. In our case, based on the experimental measurements (unloading behavior of the martensite in yy , xx and zz directions), we established $\{S_{11} \ S_{12} \ S_{13}\}$ as $\{0.022 \ -0.01 \ -0.01\} \text{GPa}^{-1}$. Using an applied stress of 250 MPa (conclusion of the plateau), the contributions of elastic strains are -0.0055 , 0.0025 , 0.0025 respectively. Then, the total, elastic, and transformation strains in our experiments are summarized below resulting in $\Delta V/V^{\text{tr}} = 0.0205$.

$$\begin{matrix} \varepsilon_{yy} \\ \varepsilon_{xx} \\ \varepsilon_{zz} \end{matrix} = \begin{Bmatrix} -0.039 \\ 0.031 \\ 0.028 \end{Bmatrix}, \begin{matrix} \varepsilon_{yy}^{\text{el}} \\ \varepsilon_{xx}^{\text{el}} \\ \varepsilon_{zz}^{\text{el}} \end{matrix} = \begin{Bmatrix} -0.0055 \\ 0.0025 \\ 0.0025 \end{Bmatrix}, \begin{matrix} \varepsilon_{yy}^{\text{tr}} \\ \varepsilon_{xx}^{\text{tr}} \\ \varepsilon_{zz}^{\text{tr}} \end{matrix} = \begin{Bmatrix} -0.0335 \\ 0.0285 \\ 0.0255 \end{Bmatrix} \Rightarrow \Delta V/V^{\text{tr}} = 0.0205 \quad (2)$$

We note that the elastic strain contribution is rather small compared to the overall strains measured (less than 2%). Our measurements show that the total strain change is 2% and the volumetric elastic strain is -0.05% resulting in a tensile transformation volumetric strain of 2.05%. These experimental procedures represent a novel approach for studying transformation strain components.

The theoretical transformation strain in [001] compression is an important measure for CoNiAl, the magnitude is $\varepsilon_{yy}^{\text{tr theory}} = -0.033$ based on our early calculations [1,2]. The experiments presented here point to $\varepsilon_{yy}^{\text{tr}} = -0.0335$. Also, the theoretical volumetric strain is reported to be of the order of 0.018 (1.8%) that is in good agreement with experiments 0.0205 (~2%).

5. Discussion of results

Stress-induced transformations have been a subject of numerous investigations and many of the basic principles of the austenite to martensite transformation are well understood. Under an imposed stress, austenite transforms to martensite, accompanied by an associated change in shape based on shear-like displacements. The reversibility of a transformation is important in cyclic loading applications, but the factors that govern this reversibility are still not well understood. For example, a volume change needs to be accommodated at the austenite and martensite interfaces and this has been suggested as an indicator of reversibility. In the case of CoNiAl, since a volume increase is associated with the transformation, tensile stress provides additional space to accommodate this volume expansion, lowering the activation energy required for the transformation. Clearly, in the case of CoNiAl the conventional wisdom associated with reversible transformation does not hold and this requires further study. This understanding is of significant importance in designing materials with improved fatigue and fracture resistance, and in shape memory applications.

We note that when the transforming region (martensite) is constrained by surrounding austenite grains, as in polycrystalline materials, the transformation shear strains hence the shape change, is reduced. In the experiments reported here, the specimens are single crystals rendering a transformation that is unconstrained producing a large macroscopic shape change. The plastic strains are insignificant in the [001] orientation. If another orientation was studied there could be individual plastic strain components, but $\Delta V/V^{\text{p}} = 0$ is expected for other cases as well.

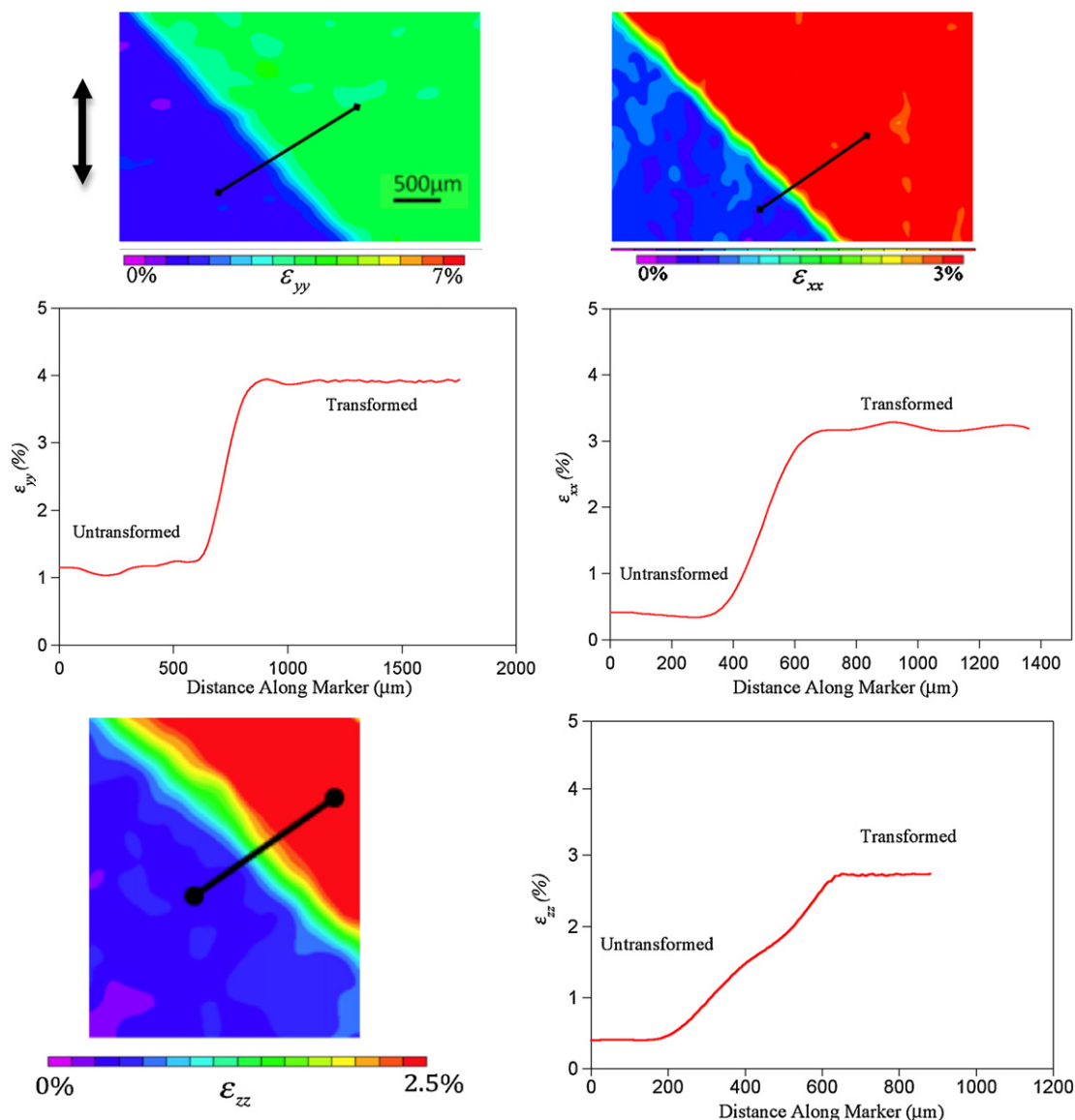


Fig. 5. Local strain measurements in untransformed and transformed regions ($\epsilon_{yy}, \epsilon_{xx}, \epsilon_{zz}$, strains); the loading direction in the images is also shown. The higher strain plateaus correspond to transformed regions and the lower strain plateaus represent the untransformed regions. In the untransformed regions the strains represent the elastic strains. Note that the strain scale differs among the three images.

Three investigations reported lattice constants for the CoNiAl to characterize the cubic to tetragonal transformation [2,3,16]. In all three cases the lattice constants result in a positive volume change, and also in our early work considerable tension-compression asymmetry has been observed consistent with the positive volume change. Admittedly, it is notable that a material with a large volumetric strain presents such a remarkable degree of recoverability. This points to rethinking some of the earlier requirements for shape memory particularly for phases that are resistant to plastic deformation and allow elastic strain accommodation. We feel that there are additional factors that need further consideration in selection and design of shape memory alloys. One of them is the difference between the M_d temperature and the A_f temperature. Microstructures, crystal lattices and heat treatments that raise the M_d temperature result in increase in slip resistance. The CoNiAl alloys exhibit an unusually high M_d temperature as evidenced by previous work [4,18]. A comparison of critical stress in compression versus temperature is made in Fig. 6 for NiTi and CoNiAl. For each case two orientations are shown, the [001] orientation is hard to slip while other orientations can undergo dislocation slip under

applied loading. The difference, $M_d - A_f$, is of the order of 500 °C in CoNiAl (Table 1 and Fig. 6) while this interval is less than 125 °C in NiTi (blue arrow). Recently, we reported an $M_d - A_f$ interval near 500 °C for multiple crystal orientations of CoNiAl (red arrow) as shown in Fig. 6 based on the results of Chumlyakov and co-workers [4,17,18]. This difference is also manifested in the lower slope of the Clausius-Clapeyron curve, measured as 1.25–3 MPa/°C for CoNiAl shown in Fig. 6 while this value is of the order of 6 MPa/°C for the 50.6%Ni–Ti alloys in Fig. 6.

Another factor, which is related, is the flow strength of the austenite and martensite phases (critical stress for dislocation slip) with respect to the transformation (austenite to martensite) stress. The critical stress for austenite exceeds 1600 MPa for the CoNiAl [001] case, and 1000 MPa for the [123] case as shown in Fig. 6. On the other hand the NiTi alloys exhibit a lower austenite stress, 1100 MPa for [001] and 700 MPa for the [112] case.

The values of volumetric transformation strain upon completion of the stress-induced transformation were found to be –0.34% in NiTi [10]. We note that there are two components influencing the tension-compression asymmetry in shape memory alloys. The

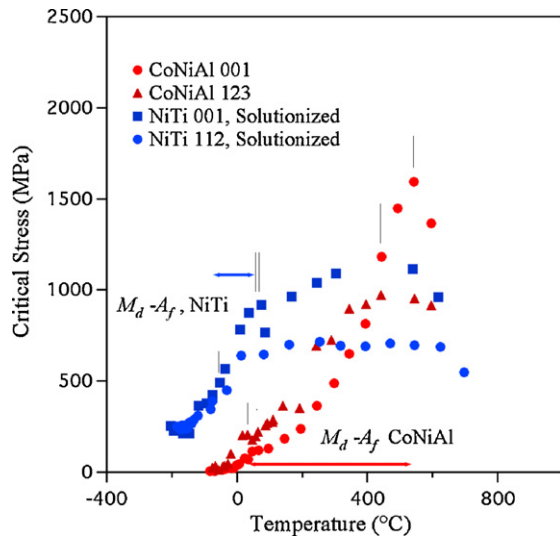


Fig. 6. Critical stress (in compression) versus temperature comparison of CoNiAl and NiTi alloys showing clearly the $M_d - A_f$ intervals for CoNiAl and NiTi. The horizontal arrows depict the $M_d - A_f$ intervals [18].

first is the low symmetry of the habit planes and the second is the volumetric strain. Depending on the habit plane direction, the tension-compression asymmetry effect due to shear can be substantial surpassing the volumetric strain effects. As the volumetric strain becomes positive, tensile loading would facilitate transformation while compressive loading will hinder transformation [17]. Many of the current models are not expected to reproduce the high levels of tensile-compressive asymmetry reported for CoNiAl alloys and this requires further consideration.

6. Conclusions

Based on experimental findings, we draw the following conclusions: The use of novel experimental techniques, and the mesoscopic resolution of the local strains in transformed and untransformed regions, allows for accurate calculation of the volumetric strains of $\sim 2\%$ in this alloy consistent with the theoretical levels of 1.8%. The axial transformation strain in compression experiments is -0.0335 , which is similar to the theoretical value of

-0.033 . Large volumetric strains do not preclude CoNiAl from pseudoelastic response with full recoverability. Factors that contribute to pseudoelasticity are the plastic slip resistance of the austenite and martensite, the high M_d temperature, and lower magnitude of transformation shear. CoNiAl possesses an exceptional high M_d temperature relative to A_f (near 500°C) compared to other shape memory alloys. Its austenite strength is also considerably higher as compared to NiTi alloys.

Acknowledgements

The work is supported by a grant from the National Science Foundation, CMMI 09-26813.

References

- [1] R.F. Hamilton, H. Sehitoglu, C. Efstathiou, H.J. Maier, Y. Chumlyakov, *Acta Materialia* 54 (2006) 587–599.
- [2] R.F. Hamilton, H. Sehitoglu, C. Efstathiou, H.J. Maier, Y. Chumlyakov, X.Y. Zhang, *Scripta Materialia* 53 (1) (2005) 131–136.
- [3] W. Maziarz, J. Dutkiewicz, L. Rogal, J. Grzonka, E. Cesari, *Journal of Microscopy* 236 (2) (2009) 143–148.
- [4] Y.I. Chumlyakov, I.V. Kireeva, E.Yu. Panchenko, I. Karaman, H. Maier, E. Cesari, V.A. Kirillov, *Russian Physics Journal* 51 (10) (2008) 1016.
- [5] K.C.M. Otsuka, *Wayman Shape Memory Materials*, Cambridge University Press, 1998.
- [6] E. Hornbogen, B. Skrotzki, *Steel Research (Germany)* 63 (8) (1992) 348–353.
- [7] J.C. Yong, S. Chu, O.O. Famodu, Y. Furuya, J. Hatrick-Simpers, R.D. James, A. Ludwig, S. Thienhaus, M. Wuttig, Z. Zhang, I. Takeuchi, *Nature Materials* 5 (4) (2006) 243–333.
- [8] R.F. Hamilton, H. Sehitoglu, H.J. Maier, Y. Chumlyakov, *Acta Materialia* 52 (2004) 3383–3402.
- [9] M. Ahlers, *Philosophical Magazine A* 82 (6) (2002) 1093–1114.
- [10] H. Sehitoglu, I. Karaman, R. Anderson, X. Zhang, K. Gall, H.J. Maier, Y. Chumlyakov, *Acta Materialia* 48 (2000) 3311–3326.
- [11] X. Zhang, H. Sehitoglu, *Materials Science and Engineering A374* (2004) 292–302.
- [12] H. Sehitoglu, I. Karaman, X. Zhang, A. Viswanath, Y. Chumlyakov, H.J. Maier, *Acta Materialia* 49 (2001) 3621–3634.
- [13] K. Gall, H. Sehitoglu, H.J. Maier, *Metallurgical Transactions 29A* (1998) 765–773.
- [14] R.F. Hamilton, H. Sehitoglu, C. Efstathiou, H.J. Maier, *Acta Materialia* 55 (14) (2007) 4867–4876.
- [15] H. Sehitoglu, X.Y. Zhang, T. Kotil, D. Canadinc, Y. Chumlyakov, H.J. Maier, *Metallurgical and Materials Transactions 33A* (2002) 3661–3672.
- [16] K. Oikawa, T. Omori, Y. Sutou, R. Kainuma, K. Ishida, *Journal de Physique IV* 112 (2003) 1017–1020.
- [17] J.R. Patel, M. Cohen, *Acta Materialia* 1 (1953) 531–538.
- [18] Y. Chumlyakov, E. Panchenko, I. Kireeva, I. Karaman, H. Sehitoglu, H.J. Maier, A. Tverdokhlebova, A. Ovsyannikov, *Materials Science and Engineering A* 481–482 (2008) 95–100.